

1.16 UTILITY OF RADIOMETRIC TEMPERATURES FOR SURFACE ENERGY FLUX ESTIMATION OF A HETEROGENEOUS DESERT ECOSYSTEM

W. P. Kustas^{1*}, J.H. Prueger², K. Ramalingam³, T.J. Schmugge¹, A. Rango¹
J.C. Ritchie¹, L.E. Hipps³ and J.L. Hatfield²

¹USDA-ARS Hydrology Lab. Beltsville, MD

²USDA-ARS Soil Tilth Lab. Ames, IA

³Dept of Plants, Soils and Biomet. Utah State Univ. Logan, UT

1. INTRODUCTION

Desert ecosystems contain sparse vegetation cover which is randomly distributed over the landscape. In many cases where shrubs have invaded primarily grassland ecosystems, it has caused a marked change in vegetation structure and distribution resulting in significant changes in surface roughness and the spatial distribution of bare soil and vegetation. Use of standard bulk similarity formulations with radiometric temperature observations for estimating energy fluxes over heterogeneous, sparsely vegetated surfaces are shown to be generally unreliable (Lhomme et al., 1997; Verhoef et al., 1997). More recent efforts have been in developing formulations that accommodate differences between radiometric and aerodynamic temperatures, and hence would be more applicable to such heterogeneous surfaces. Two such models developed by Norman et al. (1995) (referred to as N95) and Chehbouni et al. (1996) (referred to as C96) are described below which have potential of being implemented operationally with satellite data. These models are applied to data collected during JORNEX (JORNada EXperiments) over a mesquite dune site in the USDA-ARS Jornada Experimental Range near Las Cruces, New Mexico (Ritchie et al., 1996). This site contains complex topography and heterogeneous cover where 0.5 m tall honey mesquite (*Prosopis glandulosa* Torr.) vegetation grow on dunes that are 1-2 m in height and 10's of meters in width. Very little if any vegetation exists in the interspace region.

2. MODEL FORMULATIONS

For both models, turbulent transport from the surface to the lower atmosphere is based on surface layer similarity of mean profiles of temperature, T_A , and wind speed, u . In resistance form the sensible heat flux can be related to the aerodynamic temperature, T_O , as

$$H = \rho C_p \frac{(T_O - T_A)}{R_{AH}}, \quad (1)$$

where H is the sensible heat flux ($W m^{-2}$), ρC_p is the volumetric heat capacity of air ($J m^{-3} K^{-1}$), T_A is the air temperature at some reference height above the surface (K) and R_{AH} is the resistance to heat transport ($s m^{-1}$), which has the following form in the surface layer (Brutsaert, 1982):

$$R_{AH} = \frac{\left[\ln\left(\frac{z_U - d_O}{z_{OM}}\right) - \Psi_M \right] \left[\ln\left(\frac{z_T - d_O}{z_{OH}}\right) - \Psi_H \right]}{k^2 u} \quad (2)$$

In this equation, d_O is the displacement height, u is the wind speed measured at height z_U , k is von Karman's constant (≈ 0.4), z_T is the height of the T_A measurement, Ψ_M and Ψ_H are the Monin-Obukhov stability functions for momentum and heat, respectively, z_{OM} is the roughness length for momentum transport and z_{OH} is the roughness length for heat transport. T_O cannot be measured, so it is often replaced with a radiometric temperature observation at some view angle θ , $T_R(\theta)$ in Eq. (1).

In N95, a two-source approach is developed for estimating soil and vegetation contribution to the turbulent fluxes so that with an observation of $T_R(\theta)$,

$$H = \rho C_p \frac{T_R(\theta) - T_A}{R_{AR}}, \quad (3)$$

where R_{AR} is the aerodynamic-radiometric resistance,

$$R_{AR} = \frac{T_R(\theta) - T_A}{\frac{T_C - T_A}{R_{AH}} + \frac{T_S - T_A}{R_{AH} + R_S}} \quad (4)$$

Corresponding author address: W.P. Kustas, USDA-ARS Hydrology Lab., Bldg. 007, BARC-W, Beltsville, MD 20705-2350; e-mail: bkustas@hydrolab.arsusda.gov.

In Eq. (3), the resistance R_{AH} is estimated via Eq. (2), R_s is the resistance to heat transfer from the soil related to u near the soil surface (see N95), T_c and T_s are canopy and soil temperatures, respectively, and are estimated indirectly by using the Priestley-Taylor approximation for partitioning net radiation absorbed by the canopy, R_{NC} , into sensible heat flux from the canopy, H_c , and latent heat flux from the canopy, LE_c , where

$$LE_c = \alpha_{PT} f_g \frac{\Delta}{\Delta + \gamma} R_{NC} \quad (5)$$

and since $H_c = R_{NC} - LE_c$ then T_c can be solved from

$$H_c = \rho C_p \frac{T_c - T_A}{R_{AH}} \quad (6)$$

In Eq. (5), α_{PT} is the Priestley-Taylor coefficient (1.26); f_g is the fraction of green leaves; Δ is the slope of the temperature-saturation vapor pressure curve and γ is the psychrometric constant. Using an approximation between the observed radiometric temperature and soil and canopy temperatures weighted by the fraction of the field of view of the infrared radiometer occupied by canopy, $f(\theta)$,

$$T_R(\theta) \approx [f(\theta)T_c^4 + (1-f(\theta))T_s^4]^{1/4} \quad (7)$$

an estimate of T_s is obtained which can then be used to compute the sensible heat flux from the soil surface, H_s ,

$$H_s = \rho C_p \frac{T_s - T_A}{R_{AH} + R_s} \quad (8)$$

The parameter $f(\theta)$ depends upon the view zenith angle, θ , canopy type and fraction of vegetative cover, f_c . For many vegetated surfaces, assuming a random canopy with a spherical leaf angle distribution is reasonable which results in an exponential relationship with leaf area index, LAI . Closure for the energy balance of the soil and canopy is obtained from partitioning R_N between soil and vegetation as follows:

$$R_{NS} = R_N \exp(\kappa LAI) \quad (9a)$$

$$R_{NC} = R_N [1 - \exp(\kappa LAI)] \quad (9b)$$

and with a simple formulation for the soil flux, G ,

$$G = c R_{NS} \quad (10)$$

the energy balance is closed. Values of κ and c can be found in N95. The roughness parameters d_o and z_{OM} can be taken as typical fractions of the canopy height, h_c , and z_{OH} is estimated as a fraction of z_{OM} , $z_{OH} \approx z_{OM}^{1/7}$ (Brutsaert, 1982). If the estimated value of T_s is too high causing $R_{NS} - G - H_s = LE_s < 0$ (condensation during daytime conditions) then the Priestley-Taylor approximation in Eq. (5) is probably overestimating the canopy transpiration rate resulting in too low an estimate of T_c . Therefore an iteration procedure will compute LE_c values below estimates given by Eq. (5) until values of T_c and T_s in Eq. (7) compute appropriate daytime turbulent fluxes for the soil and vegetation. Further details concerning model convergence issues for the energy budgets of the soil and vegetation in later iterations and the justification for the Priestley-Taylor assumption used in Eq. (5) are given in N95. The model only requires measurements of T_A and u , $T_R(\theta)$, h_c , approximate leaf size, s , and LAI

In C96, the model computes H using Eq. (1) and a relationship for the ratio of $T_o - T_A$ and $T_R(\theta) - T_A$,

$$\beta = \frac{T_o - T_A}{T_R(\theta) - T_A} \quad (11)$$

such that Eq. (1) has the form

$$H = \rho C_p \frac{\beta(T_R(\theta) - T_A)}{R_{AH}} \quad (12)$$

The behavior of the β parameter was determined by C96 using simulations from a soil-vegetation-atmosphere model coupled to a vegetation growth model. It was found that the magnitude of β is mainly a function of LAI and is related by an expression of the form,

$$\beta = \frac{1}{\exp(L/(L-LAI)) - 1} \quad (13)$$

where L was empirically determined ($L \approx 1.5$). In C96, R_{AH} in Eq. (12) is computed from Eq. (2), but with $z_{OH} = z_{OM}$.

3. THE DATA

In May of 1995 a Radiation and Energy Balance Systems** (REBS) Bowen ratio (BR) station was erected at

the mesquite dune site and ran continuously until January of 1997. The BR tower was located on top of a large dune with the measurements of temperature and humidity at approximately 2 and 4 m above the interdunal surface elevation and u and R_N measured at approximately 4.5 m. The soil heat flux was estimated with 3 heat flow plates at -0.05 m and averaging soil temperature sensors for the layer above the plates for computing heat storage (Brutsaert, 1982). Net radiation was measured with a REBS model Q7.1 and wind speed was measured with a MET One 3-cup anemometer having a 0.3 m s^{-1} threshold.

In May of 1996, a 10 meter tower was erected approximately 70 m south of the BR station. The tower was instrumented with sensors to measure air temperature, vapor pressure, and wind speed at 3, 4, 5, 6, 8, and 10 m above the surface. Surface temperatures were estimated using 2 Everest Infrared Temperature Transducers (IRTs; Model 4000) located at the top of the 10 m tower. The IRTs had a 60° field of view (FOV) and were oriented to the north and south having 45° view angles. Net radiation was estimated with a REBS Q7.1 located at 10 m and oriented in a southern direction. For the 10 m tower measurements, 30 minute average output was recorded.

For approximately a week in September 1995, May 1996, and September 1996 a set of intensive measurements were made (Ritchie et al., 1996). These included H and LE fluxes estimated nominally at a height of 3 m above the surface on a tower using eddy covariance, EC. A Campbell Scientific Inc. (CSI) 1-D sonic anemometer and fine wire thermocouple and CSI Krypton hygrometer were used. The sampling frequency for the CSI EC system was 10 Hz with fluxes averaged every 30 minutes.

Hand-held IRT measurements using Everest Model 110/130 instruments having 3° or 15° FOV were made over a $25 \times 25 \text{ m}$ grid containing dune and interdune areas. Approximately 30 IRT observations were recorded over the grid which took between 10 and 20 minutes to complete. Measurements were usually made between 9 and 14 Mountain Standard Time (MST). Measurements with a nadir viewing Everest IRT having a 15° FOV were also collected from an aircraft flying 120 to 300 m above the surface.

Estimates of LAI were made during the May and September field campaigns using the LiCor LAI-2000. Measurements were made in the dune area along a 150 m transect with three 30 m segments where measurements were made every meter and two 30 m gaps where no measurements were collected. Measurements were also made in February when no leaves are present on the mesquite. Typically March through May is relatively dry with most precipitation occurring during the "wet" season (July-September) and the winter months. The honey mesquite leafs out in the spring. Values of LAI for observations in February, May and September of 1996 were ≈ 0.5 while $LAI \approx 0.75$ for September 1995. The

annual precipitation for 1995 and 1996 was 30% below the long term average ($\approx 240 \text{ mm}$) and are therefore considered drought years. The fact that LAI values changed little from the baseline measurements made in February indicates a small amount of green leaf vegetation was present for May and September 1996 and that the mesquite branches/stems were mainly responsible for attenuating radiation. The higher LAI value for September 1995 probably is the result of some significant precipitation occurring during the winter months recharging the mesquite root zone and significant precipitation during the wet season increasing the presence of interdune vegetation.

4. PRELIMINARY RESULTS

Preliminary results will first be presented using the ground-based hand-held IRT data collected in September '95 (S95) and September '96 (S96) and May '96 (M96) and with meteorological data from the BR tower for model input. Additional data from the tower during M96 and S96 will be used to test model sensitivity to a change in the LAI estimate. Preliminary analysis of the flux data (Hippis et al., 1997) indicates that the BR method has difficulty resolving vapor pressure gradients over this site, and therefore comparisons between modeled and measured fluxes are made only with the EC technique.

An example of the the hand-held IRT measurements from M96 of the mesquite and interdune vegetation versus interdune bare soil and mixtures of mesquite dune and bare soil areas is illustrated in Figure 1. The plot indicates that temperature differences between vegetation and bare soil can reach $15\text{-}20^\circ \text{ C}$.

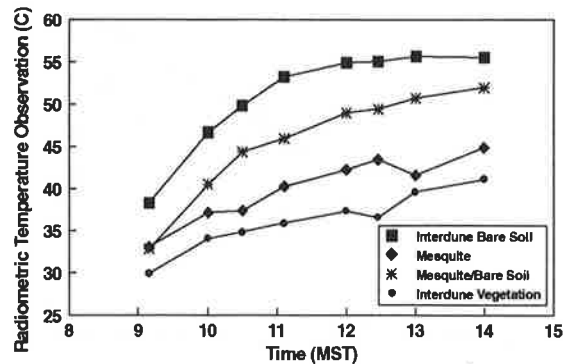


Figure 1. An example of hand-held radiometric temperature observations of vegetation, bare soil and mixtures of bare soil and mesquite (mesquite/bare soil).

Video imagery modified to contrast the mesquite dunes from the interdune areas indicate $f_c \approx 0.3$ (Figure 2). The clumpiness of the vegetation is also quite apparent which probably requires replacing LAI in Eq. (9) and (13) with ΩLAI where Ω is a clumping factor (Chen and Cihlar,

1995). An estimate of Ω will be applied in future analyses.

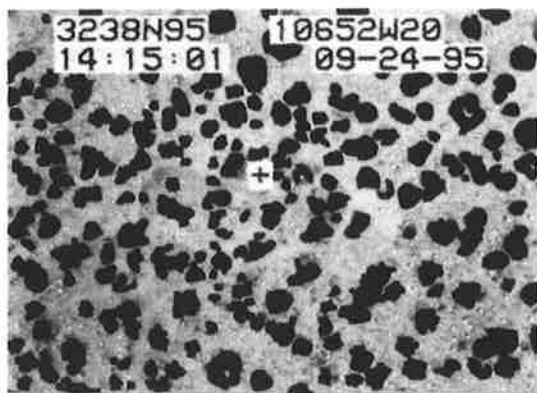


Figure 2. Video imagery near BR station modified to highlight mesquite dunes (i.e., dark features).

By weighting the radiances of canopy and soil temperatures from hand-held observations with the estimate of f_c , a composite $T_R(\theta)$ was estimated and compared to $T_R(\theta)$ from the tower (≈ 35 m pixel) and from the aircraft with a 30-80 m pixel size depending on aircraft altitude (Figure 3). Differences in $T_R(\theta)$ between the tower and hand-held gave a root-mean-square-error (RMSE) of 0.9° while for the aircraft, which had higher $T_R(\theta)$ values, RMSE $\approx 3^\circ$. Larger differences and higher $T_R(\theta)$ values from aircraft is likely due to the more significant influence of bare soil temperatures with the nadir observations. A regression equation forced through the origin between the average of north and south viewing $T_R(\theta)$ from the tower and the hand-held observations resulted in a slope of 0.99.

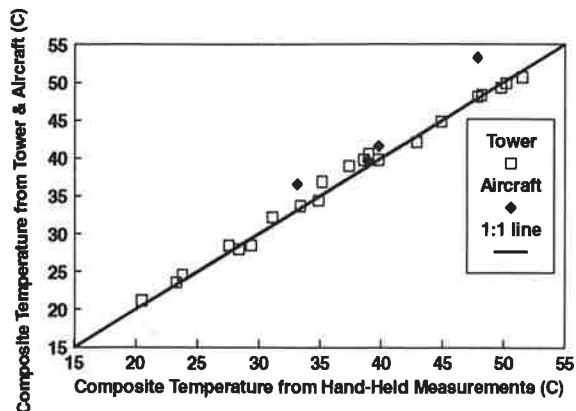


Figure 3. Comparison of composite $T_R(\theta)$ estimated from hand-held measurements versus tower and aircraft observations.

Neutral wind profiles from the tower were used for estimating d_0 and z_{OM} for the site and yielded values of $d_0 \approx 1$ m and $z_{OM} \approx 0.07$ m. For the N95 model, $h_c = 1.75$ m, $s = 0.01$ and $LAI = 0.75$ for S95 and $LAI = 0.5$ for M96 and

S96. Gibbons et al (1996) estimated a LAI for mesquite leaves, LAI_{LEAF} , ≈ 0.3 from the dune areas during 1991 and 1992, both wet years where annual rainfall exceeded the average by 60% and 30%, respectively. Assuming that $LAI_{LEAF} \approx 1/4$ of the wet year value for M96 and S96 then f_g was estimated from the ratio LAI_{LEAF}/LAI ($0.075/0.5$) ≈ 0.15 for M96 and S96. For S95, $LAI_{LEAF} \approx 0.25$, which was estimated by subtracting the total LAI (0.75) from the "baseline" value (≈ 0.5) yielding $f_g \approx 0.3$ for S95. For the C96 model, LAI was assigned the same values of 0.5 for M96 and S96 and 0.75 for S95.

In Figure 4 are comparisons between H predicted by C96 and N95, respectively, and measurements of H using the EC technique. The N95 model performs well for all

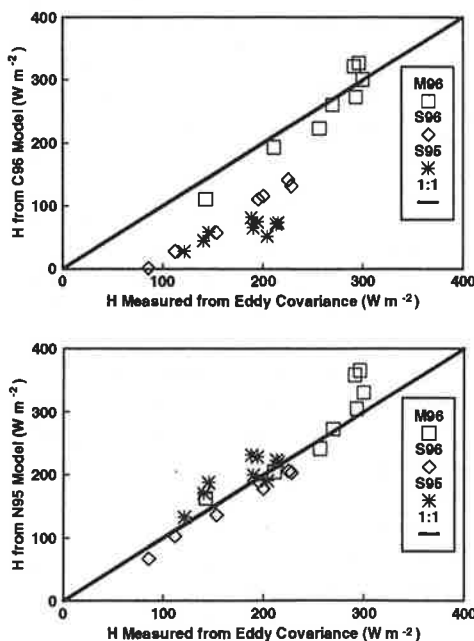


Figure 4. Comparison of H predicted by C96 and N96 models versus H measured by EC technique for M96, S96 and S95 campaigns.

three periods while C96 significantly underestimates S96 and S95 periods. The RMSE ≈ 90 $W m^{-2}$ for C96 while RMSE ≈ 30 $W m^{-2}$ for N95. The N95 model also predicts LE which is compared to the EC measurements in Figure 5. In the case of LE , the N95 model overpredicts LE for most of the observations in M96 and all of S95 with the resulting RMSE ≈ 55 $W m^{-2}$.

Additional data from the tower collected during M96 and S96 campaigns were also used to run both models. Fluxes were estimated using T_A and u observations for all six levels. Kustas et al. (1997) found roughness sublayer effects on flux-gradient relationships at almost all measurement levels, but that this effect was not strongly evident when using integrated forms of Monin-Obukhov surface layer similarity equations with surface temperature as the

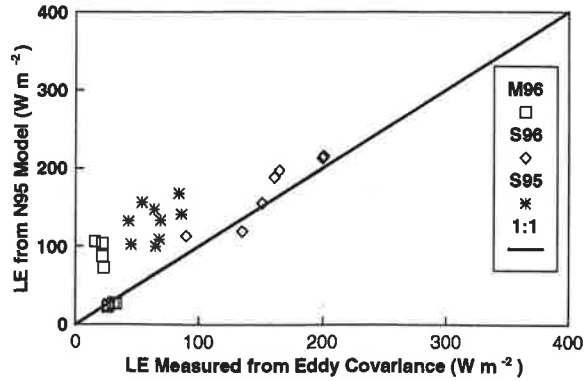


Figure 5. Comparison of LE predicted by N95 model versus LE measured by EC technique for the M96, S96 and S95 campaigns.

boundary condition. The predictions of H by C96 showed some dependency with height of u and T_A observations ranging from a maximum of $\approx 35 \text{ W m}^{-2}$ between 3 m and 10 m to $\approx 5 \text{ W m}^{-2}$ between 8 m and 10 m. For the N95 model, differences between levels showed no real dependency, which averaged $\approx 2 \text{ W m}^{-2}$.

Averages of H predictions from all six levels is shown in Figure 6. The C96 model tends to underpredict H yielding a RMSE $\approx 56 \text{ W m}^{-2}$ while the N95 model has a slight tendency to overpredict H , but in general is in good agreement with the EC data yielding RMSE $\approx 30 \text{ W m}^{-2}$.

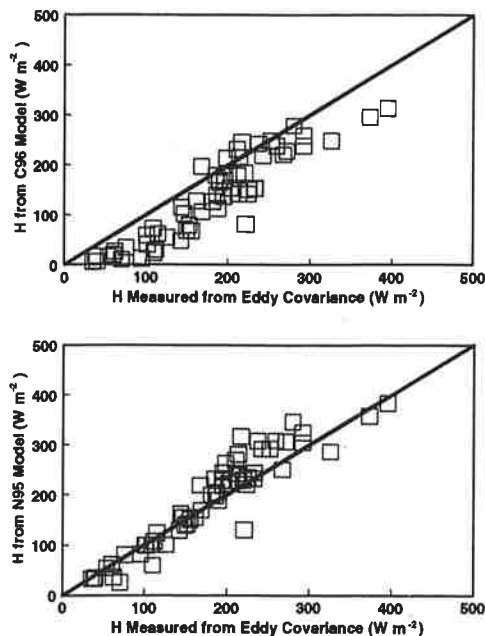


Figure 6. Comparison of H predicted by C96 and N95 models using tower data versus H measured by EC technique for M96 and S96 campaigns.

For LE , the N95 model predictions mostly fall along the 1:1

line (Figure 7) except for a group of observations where N95 overpredicts observed LE by 50-100 W m^{-2} . These overpredictions were from a day with unsteady conditions which eventually resulted in convective precipitation over the dune site.

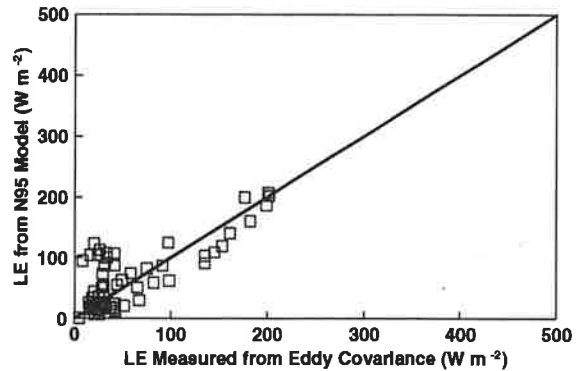


Figure 7. Comparison of LE predicted by N95 model using tower data versus LE measured by EC technique for M96 and S96 campaigns.

5. CONCLUSIONS

Both C96 and N95 models consider factors that cause differences between T_o and $T_R(\theta)$ and therefore represent an advance over models which ignore such affects. Differences between T_o and $T_R(\theta)$ are pronounced for sparse canopy covered surfaces and so are an issue for desert ecosystems. However, LAI is a critical parameter in these and other two-source models and is difficult to define or determine over heterogeneous surfaces. Moreover, given the spatial distribution of shrub vegetation in desert ecosystems, a clumping factor Ω may need to be included in these model formulations.

There is a high correlation between the tower $T_R(\theta)$ and the hand-held observations suggesting off nadir ($\theta \approx 45^\circ$) may provide more reliable composite temperatures for these heterogeneous surfaces than given by nadir observations. Therefore $T_R(\theta)$ from a satellite platform may provide better estimates of composite surface temperatures at off nadir view angles over desert ecosystems.

This preliminary study indicates that the accuracy of C96 and N95 model predictions of H and LE fluxes for this ecosystem largely depends on how LAI is defined and for N95, estimating an appropriate f_g . Although remotely sensed vegetation indices (VIs) are related to the amount of LAI , VIs are strongly affected by soil background and canopy structure making these indices difficult to use in desert environments. VIs are mainly affected by the amount of green vegetation present, so it is speculated that a remotely sensed estimate of LAI for this dune area would be representative of LAI_{LEAF} .

Using the S96 and M96 tower data with $LAI = LAI_{LEAF} = 0.075$ and $f_g = 1$, the predictions of H with C96 and N95 models are shown in Figure 8. The results with the C96 model suggest this model will be sensitive to how LAI is defined or estimated and that the parameter L in Eq. (13) may need to be modified depending on vegetation type and structure and possibly on how the vegetation cover is distributed. The N95 model tends to underpredict the observed H but without a significant increase in scatter from Figure 6. This bias in H , however, causes an increase in RMSE for H to approximately 50 W m^{-2} and a larger bias in the estimate of LE with RMSE increasing to $\approx 57 \text{ W m}^{-2}$ (Figure 9).

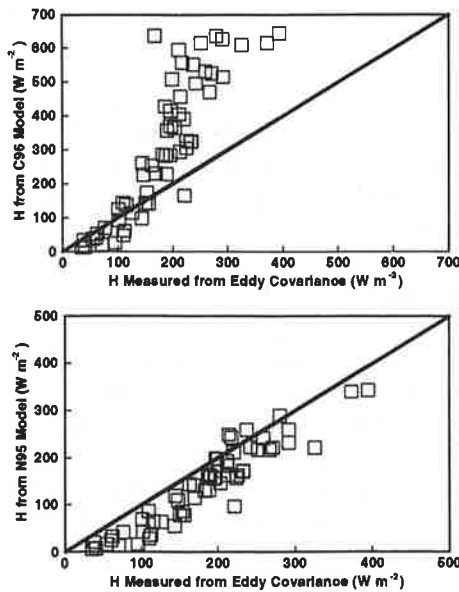


Figure 8. Comparison of H predicted by C96 and N95 models using tower data and $LAI = LAI_{LEAF} = 0.075$ versus H measured by EC technique for M96 and S96 campaigns.

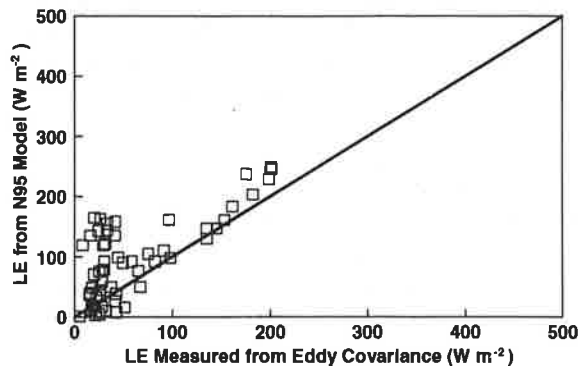


Figure 9. Comparison of LE predicted by N95 model using tower data and $LAI = LAI_{LEAF} = 0.075$ versus LE measured by EC technique for M96 and S96 campaigns.

6. REFERENCES

- Brutsaert, W. 1982. *Evaporation into the Atmosphere*. D. Reidel Pub. Co. Dordrecht, Holland. 299pp.
- Chebouni, A. et al., 1996. Examination of the difference between radiative and aerodynamic surface temperatures over sparsely vegetated surfaces. *Remote Sens. Environ.* **58**:177-186.
- Chen, J.M., and J. Cihlar, 1995. Quantifying the effect of canopy architecture on optical measurements of leaf area index using two gap size methods. *IEEE Trans. Geosci. Remote Sens.* **33**:777-787.
- Gibbens, R.P. et al., 1996. Structure and function of C_3 and C_4 Chihuahuan Desert plant communities. Standing crop and leaf area index. *J. Arid Environ.* **34**: 47-62.
- Hipps, L.E. et al., 1997. Surface fluxes and energy balance in an arid ecosystem. *AMS Preprint 12th Symp. Boun.-Layer & Turb.* pp. 553-554.
- Kustas, W.P. et al., 1997. Application of surface layer similarity theory in a heterogeneous desert ecosystem. *AMS Preprint 12th Symp. Boun.-Layer & Turb.* pp. 277-278.
- Lhomme, J.-P. et al., 1997. Sensible heat flux and radiometric temperature over sparse Sahelian vegetation II. A model for the kB^{-1} parameter. *J. Hydrol.* **188-189**:839-854.
- Norman J.M. et al., 1995. A two-source approach for estimating soil and vegetation energy fluxes from observations of directional radiometric surface temperature. *Agric. For. Meteorol.* **77**: 263-293.
- Ritchie, J.C. et al., 1996. An airborne campaign to quantify rangeland vegetation change and plant community - atmosphere interactions. *Proc. Inter. Airborne Remote Sens. Conf.* **2**:54-66.
- Verhoef, A. et al, 1997. Some practical notes on the parameter kB^{-1} for sparse vegetation. *J. Appl. Meteorol.* **36**: 560-572.

**Company and trade names are given for the benefit of the reader and imply no endorsement by the USDA.